Biophysical Chemistry 136 (2008) 32–37

Contents lists available at ScienceDirect

Biophysical Chemistry

journal homepage: http://www.elsevier.com/locate/biophyschem

System-size resonance for intracellular and intercellular calcium signaling

Ying Wang [a,b], Qianshu Li [a,c,*]

[a] The Institute for Chemical Physics, Beijing Institute of Technology, Beijing, 100081, PR China
[b] Department of Chemistry, Sichuan University of Science and Engineering, Sichuan, 643000, PR China
[c] Center for Computational Quantum Chemistry, South China Normal University, Guangzhou, 510006, PR China

ARTICLE INFO

Article history:
Received 5 December 2007
Received in revised form 10 April 2008
Accepted 10 April 2008
Available online 18 April 2008

Keywords:
Synchronization
Chemical Langevin method
Coupling strength
Internal noise

ABSTRACT

Dynamical behaviors of unidirectionally, linearly coupled as well as isolated calcium subsystems are investigated by taking into account the internal noise resulting from finite system size and thus small numbers of interacting molecules. For an isolated calcium system, the internal noise can induce stochastic oscillations for a steady state close to the Hopf-bifurcation point, and the regularity of those stochastic oscillations depends resonantly on the system size, exhibiting system-size resonance. For the coupled system consisting of two subsystems, the system-size resonance effect observed in the subsystem subject to coupling is significantly amplified due to the nontrivial effects of coupling.

1. Introduction

In recent years, the influence of internal fluctuations on intrinsic dynamics has been intensively studied in biochemical processes, such as in calcium signaling [1–3], genetic regulations [4], circadian rhythms [5], and neuron spikings [6,7]. The investigation of internal fluctuations in nonlinear systems has led to the emergence of novel concepts such as system-size resonance (SSR). So far, mainly two types of SSR have been reported. One is that the behavior of an array of coupled noisy dynamical elements is the most ordered when the number of elements is optimal [8–10]. The other is that internal noise originating from the random fluctuations in finite-size biochemical systems are used to extract coherent signals and there are the strongest periodicities at a certain system size [11–13]. For instance, ion channel clusters of optimal sizes can enhance the encoding of a subthreshold stimulus [11], and optimal intracellular calcium signaling appears at a certain size or distribution of the ion channel clusters [12,13]. Recently, there has been increasing interests in coupled oscillators. Especially interesting is the phenomenon of array-enhanced coherence resonance (AECR), where the coherence can be significantly improved when the noisy excitable elements are coupled [14–16]. The influence of internal noise has been taken into account in coupled oscillators in biosystems [17–19]. For example, conductance noise induces frequency and phase synchronization in populations of weakly coupled neurons [17]. Internal noise resulting from finite system size makes the doublets of calcium oscillators synchronized [18,19]. Intercellular calcium signals are propagated in multicellular hepatocyte systems as well as in the intact liver. Some interhepatocyte Ca^{2+} signals are unidirectional for a given agonist [20]. However, little work has been done forward the understanding of the influences of coupling on the SSR phenomenon.

As the second messenger, calcium ions play an important role in a variety of cell types. Their oscillations control the birth, life, death of cell, tune the living process of cell, and enhance the efficiency and specificity of gene expression [21]. Calcium ion is therefore an integral part of the information-processing machinery in living organisms, and its diverse functions have been studied intensively [22–24]. Moreover, SSR phenomena have been achieved in calcium systems [1,2]. Nevertheless, to the best of our knowledge, influences of coupling on the SSR behavior in calcium system have gained a little insight. While many models have been developed to explain calcium oscillations, most of these models focus on the simple periodic oscillations [25,26] and only a few models are able to display complex periodic oscillations.

In this research, the Kummer model [27] was adopted to gain more insight into the influence of internal noise. This model is capable of displaying both simple and complex dynamic behavior [27]. By constructing a mesoscopic stochastic model, calculations show that the internal noise originating from finite system size is able to extract an inherent periodic signal of the system in a resonant manner at the point close to the supercritical Hopf bifurcation, indicating the occurrence of SSR. Additionally, the

* Corresponding author. The Institute for Chemical Physics, Beijing Institute of Technology, Beijing, 100081, PR China. Tel./fax: +86 10 6891 2665.
E-mail address: qsli@bit.edu.cn (Q. Li).

0301-4622/$ – see front matter © 2008 Elsevier B.V. All rights reserved.
doi:10.1016/j.bpc.2008.04.003

phenomenon of the SSR also appears in the periodic bursting regime due to the influence of internal noise. Later, two such calcium systems are coupled unidirectionally to explore how the SSR behavior changes with the variation of the coupling strength. It was found that SSR behavior still exists in each subsystem in the presence of coupling, and the SSR effect of the subsystem is significantly enhanced by increasing the coupling strength. This is an essential difference from the work done by Xin et al. [28], where the subsystems are bidirectionally coupled.

2. Model description

The model used here is able to display simple and complex behavior of calcium, depending on the kinetics of the receptor complex i.e., the agonist-specific receptor [29]. After the binding of an agonist to the extracellular side of a membrane-bound receptor molecule, the G_α subunit at the intracellular side of the receptor-coupled G-protein is activated. The activated G-protein in turn stimulates a phospholipase C (PLC), which leads to the production of IP_3, which diffuses through the cell and binds to receptors at the endoplasmic reticulum (ER). This leads to the liberation of calcium ion from endoplasmic reticulum and in some cases to the inflow of calcium ion from extracellular space [27]. The model of a single cell can be described by the following equations:

$$\begin{aligned}
\frac{dw}{dt} &= k_1 + k_2 w - \frac{k_3 w x}{w + K_4} - \frac{k_5 w x}{w + K_6},\\
\frac{dx}{dt} &= k_7 w - \frac{k_8 x}{x + K_9},\\
\frac{dy}{dt} &= \frac{k_{10} x y z}{z + K_{11}} + k_{12} x + k_{13} w - \frac{k_{14} y}{y + K_{15}} - \frac{k_{16} y}{y + K_{17}},\\
\frac{dz}{dt} &= -\frac{k_{10} x y z}{z + K_{11}} + \frac{k_{16} y}{y + K_{17}},
\end{aligned} \tag{1}$$

where w denotes the concentration of active G_α subunits of the G-protein, which are responsible for the activation of PLC. $\underline{x}$ refers to the concentration of active PLC. $\underline{y}$ is the concentration of free calcium ions in the cytosol, and $\underline{z}$ denotes the concentration of calcium in the ER. More details of the model can be found in Ref. [27]. Parameter values used in this study are: $k_1=0.09$, $k_3=0.64$, $k_4=0.19$, $k_5=4.88$, $k_6=1.18$, $k_7=2.08$, $k_8=32.24$, $k_9=29.09$, $k_{10}=5.0$, $k_{11}=2.67$, $k_{12}=0.7$, $k_{13}=13.58$, $k_{14}=153.0$, $k_{15}=0.16$, $k_{16}=4.85$, and $k_{17}=0.05$. $\underline{k_2}$ is the concentration of the agonist and is selected as the control parameter.

Deterministic equations could correctly describe the dynamics of the processes that involve macroscopically large quantities. When using the deterministic equations, one computes continuous concentrations of the participating species. However, biochemical reactions in the cell involve only a small number of molecules due to small cell volume. Interactions of a small number of molecules demand a stochastic approach, because internal fluctuations cannot be neglected anymore [30]. Biochemical reactions in the cell are governed by a chemical master equation, which is the basis for chemical simulation, but difficult to be solved analytically. The exact stochastic simulation algorithm introduced by Gillespie [31] has been widely used, which stochastically determines what the next reaction step is and when it will happen according to the transition probability of each reaction step. It has to be addressed that this model is a simplified one and does not include all the processes that are know to occur in the calcium system. However, the basic dynamical characteristics are caught in this model. Furthermore, in Kummer's following work, he has used the exact stochastic simulation (ESS) method to perform stochastic simulation with the core model [29]. In accordance with ESS method, the number of active G_α units is introduced as $\underline{W}$, the number of active PLC as $\underline{X}$, the number of calcium ions in the cytosol as $\underline{Y}$, and the number of calcium ions in the ER as $\underline{Z}$. As is described in Ref. [27], the model was constructed on the basis of previous experimental observations and data like those shown in Figs. 1 and 2 in Ref. [27], where the quantity is between 0 and 1000, and the unit of the calcium concentration is nM. In the present work, the results of calcium concentration by deterministic simulations are between 0 and 10. Therefore, the unit μM for concentration and μm^3 for the volume are chosen to give qualitative discussion. The concentration of the reactants are $w=\frac{\frac{W}{L}\times 10^6}{V\times 10^{-15}}=\frac{W}{VL}\times 10^{21}(\mu M)$, $x=\frac{X}{VL}\times 10^{21}(\mu M)$, $y=\frac{Y}{VL}\times 10^{21}(\mu M)$ and $z=\frac{Z}{VL}\times 10^{21}(\mu M)$, where L is the Avogadro's number. The volume $\underline{V}$ is used to convert concentrations into numbers of molecules and then regulate the intensity of internal noise. According to the model biochemical reactions in the cell can be grouped into eleven processes for the current model, and the corresponding transition probabilities for the processes are listed in Table 1. $a_1 \ldots a_{11}$ are transition rates, as are described in Table 1, where several reaction progresses have been eliminated according to the deterministic model.

The exact stochastic simulation algorithm can account for the internal noise exactly, but it is too time consuming when the system size is large. The chemical Langevin (CL) method [32] has proven to be an efficient simulation algorithm [33–35] to take internal noise into account if a macro-infinitesimal time scale exists in the system. CL equations for the current model are described as

$$\begin{aligned}
\frac{dW}{dt} &= (a_1 + a_2 - a_3 - a_4) + (\sqrt{a_1}\xi_1 + \sqrt{a_2}\xi_2 - \sqrt{a_3}\xi_3 - \sqrt{a_4}\xi_4),\\
\frac{dX}{dt} &= (a_5 - a_6) + (\sqrt{a_5}\xi_5 - \sqrt{a_6}\xi_6),\\
\frac{dY}{dt} &= (a_7 + a_8 + a_9 - a_{10} - a_{11})\\
&\quad + (\sqrt{a_7}\xi_7 + \sqrt{a_8}\xi_8 + \sqrt{a_9}\xi_9 - \sqrt{a_{10}}\xi_{10} - \sqrt{a_{11}}\xi_{11}),\\
\frac{dZ}{dt} &= (a_{11} - a_7) + (\sqrt{a_{11}}\xi_{11} - \sqrt{a_7}\xi_7).
\end{aligned} \tag{2}$$

Where $\xi_{i=1,\ldots,11}(t)$ are Gaussian white noises with $\langle \xi_i(t)\rangle = 0$ and $\langle \xi_i(t)\xi_j(t')\rangle = \delta_{ij}\delta(t-t')$. $a_1 \ldots a_{11}$ are transition rates, as are described in Table 1, where several reaction progresses have been eliminated according to the deterministic model. According to the relationship

Table 1
Stochastic transition processes and corresponding rates

Transition processes	Description	Transition rates
(1)$W\to W+1$	The spontaneous activation of G_α units	$a_1=V\cdot k_1$
(2)$W\to W+1$	The accelerated formation of active G_α after binding of agonist to the membrane receptor	$a_2=V\cdot k_2 w$
(3)$W\to W-1$	The inactivation of G_α units accelerated by active PLC	$a_3 = V\cdot\frac{k_3 w x}{w+K_4}$
(4)$W\to W-1$	Negative feedback of calcium-dependent kinase on G_α units	$a_4 = V\cdot\frac{k_5 w x}{w+K_6}$
(5)$X\to X+1$	The activation of PLC depends on the concentration of active G_α units	$a_5=V\cdot k_7 w$
(6)$X\to X-1$	The enzymatic inactivation of PLC	$a_6 = V\cdot\frac{k_8 x}{x+K_9}$
(7)$Y\to Y+1$ $Z\to Z-1$	The inflow of calcium from the internal stores	$a_7 = V\cdot\frac{k_{10} x y z}{z+K_{11}}$
(8)$Y\to Y+1$	The influx of calcium from the extracellular Space stimulated by IP_3	$a_8=V\cdot k_{12} x$
(9)$Y\to Y+1$	The influx of receptor-operated calcium	$a_9=V\cdot k_{13} w$
(10)$Y\to Y-1$	The pump of cytosol Ca^{2+} into the ER by ATP-dependent pumps	$a_{10} = V\cdot\frac{k_{14} y}{y+K_{15}}$
(6)$Y\to Y-1$ $Z\to Z+1$	The pump of cytosol Ca^{2+} into the extracellular space by ATP-dependent pumps	$a_{11} = V\cdot\frac{k_{16} y}{y+K_{17}}$

between the concentration and the molecule number, the corresponding macroscopic differential equations for the CL equations read

$$\begin{aligned}
\frac{dw}{dt} &= \left(k_1 + k_2 w - \frac{k_3 wx}{w+K_4} - \frac{k_5 wx}{w+K_6}\right) \\
&\quad + \frac{1}{\sqrt{V}}\left(\sqrt{k_1}\xi_1 + \sqrt{k_2 w}\xi_2 - \sqrt{\frac{k_3 wx}{w+K_4}}\xi_3 - \sqrt{\frac{k_5 wx}{w+K_6}}\xi_4\right), \\
\frac{dx}{dt} &= \left(k_7 w - \frac{k_8 x}{x+K_9}\right) + \frac{1}{\sqrt{V}}\left(\sqrt{k_7 w}\xi_5 - \sqrt{\frac{k_8 x}{x+K_9}}\xi_6\right), \\
\frac{dy}{dt} &= \left(\frac{k_{10}xyz}{z+K_{11}} + k_{12}x + k_{13}w - \frac{k_{14}y}{y+K_{15}} - \frac{k_{16}y}{y+K_{17}}\right) + \frac{1}{\sqrt{V}}\left(\sqrt{\frac{k_{10}xyz}{z+K_{11}}}\xi_7\right. \\
&\quad \left. + \sqrt{k_{12}x}\xi_8 + \sqrt{k_{13}w}\xi_9 - \sqrt{\frac{k_{14}y}{y+K_{15}}}\xi_{10} - \sqrt{\frac{k_{16}y}{y+K_{17}}}\xi_{11}\right), \\
\frac{dz}{dt} &= \left(\frac{k_{16}y}{y+K_{17}} - \frac{k_{10}xyz}{z+K_{11}}\right) + \frac{1}{\sqrt{V}}\left(\sqrt{\frac{k_{16}y}{y+K_{17}}}\xi_{11} - \sqrt{\frac{k_{10}xyz}{z+K_{11}}}\xi_7\right).
\end{aligned} \tag{3}$$

From the form of Eq. (3) it can be found that the level of internal noise in the studied system is proportional to $1/\sqrt{V}$. If $V\to\infty$, Eq. (3) is equal to the deterministic Eq. (1).

If two subsystems are coupled unidirectionally, the form of Eq. (3) is invariable for the first subsystem but for the second subsystem the third equation in CL Eq. (3) is expressed as the following to reflect the coupling effect

$$\begin{aligned}
\frac{dy_2}{dt} &= \left(\frac{k_{10}x_2y_2z_2}{z_2+K_{11}} + k_{12}x_2 + k_{13}w_2 - \frac{k_{14}y_2}{y_2+K_{15}} - \frac{k_{16}y_2}{y_2+K_{17}}\right) \\
&\quad + \frac{1}{\sqrt{V}}\left(\sqrt{\frac{k_{10}x_2y_2z_2}{z_2+K_{11}}}\xi_7 + \sqrt{k_{12}x_2}\xi_8 + \sqrt{k_{13}w_2}\xi_9 - \sqrt{\frac{k_{14}y_2}{y_2+K_{15}}}\xi_{10}\right. \\
&\quad \left. - \sqrt{\frac{k_{16}y_2}{y_2+K_{17}}}\xi_{11}\right) + g(y_1 - y_2),
\end{aligned} \tag{4}$$

where g is the coupling strength. Indices 1 and 2 refer to the first or the second subsystem.

3. Results and discussion

In order to elucidate the effects of internal noise on the calcium system, it is necessary to study the corresponding deterministic kinetics as comparison. In this study, we are primarily interested in the steady state and the limit cycle dynamics. Eq. (1) is integrated by using the forward Euler method with a time step of 0.0005 s. Fig. 1 is the bifurcation diagram of y as a function of k_2 being varied from 0 to 1.7. As seen in Fig. 1, with the variation of the control parameter k_2, the calcium system undergoes a Hopf bifurcation (HB) at $k_2 \approx 1.13$. Close to the onset of oscillations, the amplitude is small, and the bifurcation is expected for a supercritical Hopf bifurcation. Above HB the system shows limit cycle behavior and below HB the system is at steady state. With further increase of the control parameter k_2, the calcium response switches to complex periodic oscillations and finally yields chaotic oscillations [27].

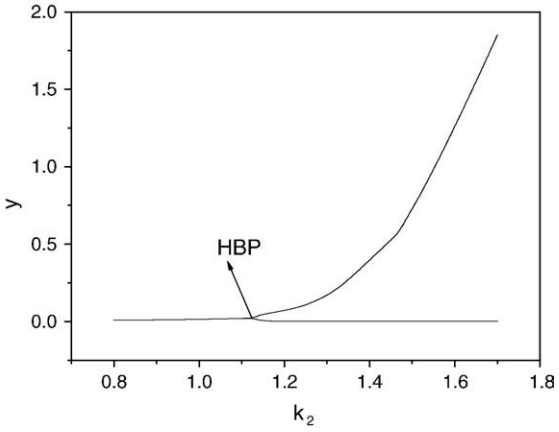

Fig. 1. Bifurcation diagram for y at $0<k_2<1.7$. The bifurcation value is about 1.13.

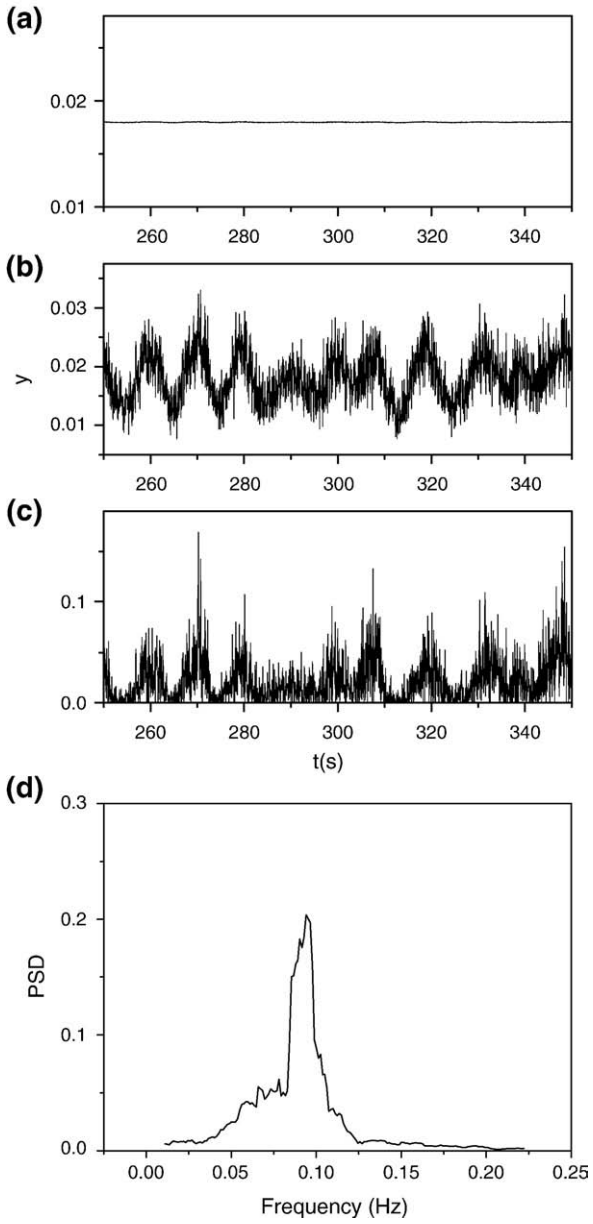

Fig. 2. Temporal courses for y at various volumes. (a) $V=10^2$ μm^3, (b) $V=10^4$ μm^3, (c) $V=10^7$ μm^3, (d) The power spectrum density (PSD) for $V=10^4$ μm^3.

It is well known that living cells involve a small number of interacting molecules owing to their finite volumes, hence, the state of the system is discrete and deterministic equations may give misleading results. We tune the control parameter k_2 to 1.06 which is in the vicinity of HB, and simulate the dynamics via solving the mesoscopic CL Eq. (3) to account for the intrinsic noise. Temporal courses of y at different volumes are presented in Fig. 2a–c, Fig. 2a for $V=10^2$ μm^3, Fig. 2b for $V=10^4$ μm^3 and Fig. 2c for $V=10^7$ μm^3. Numerical calculations are performed by the Eular–Maruyama method [36] with a time step of 0.0005 s. When the system size V is large, the stochastic simulation approaches the deterministic limit, and the

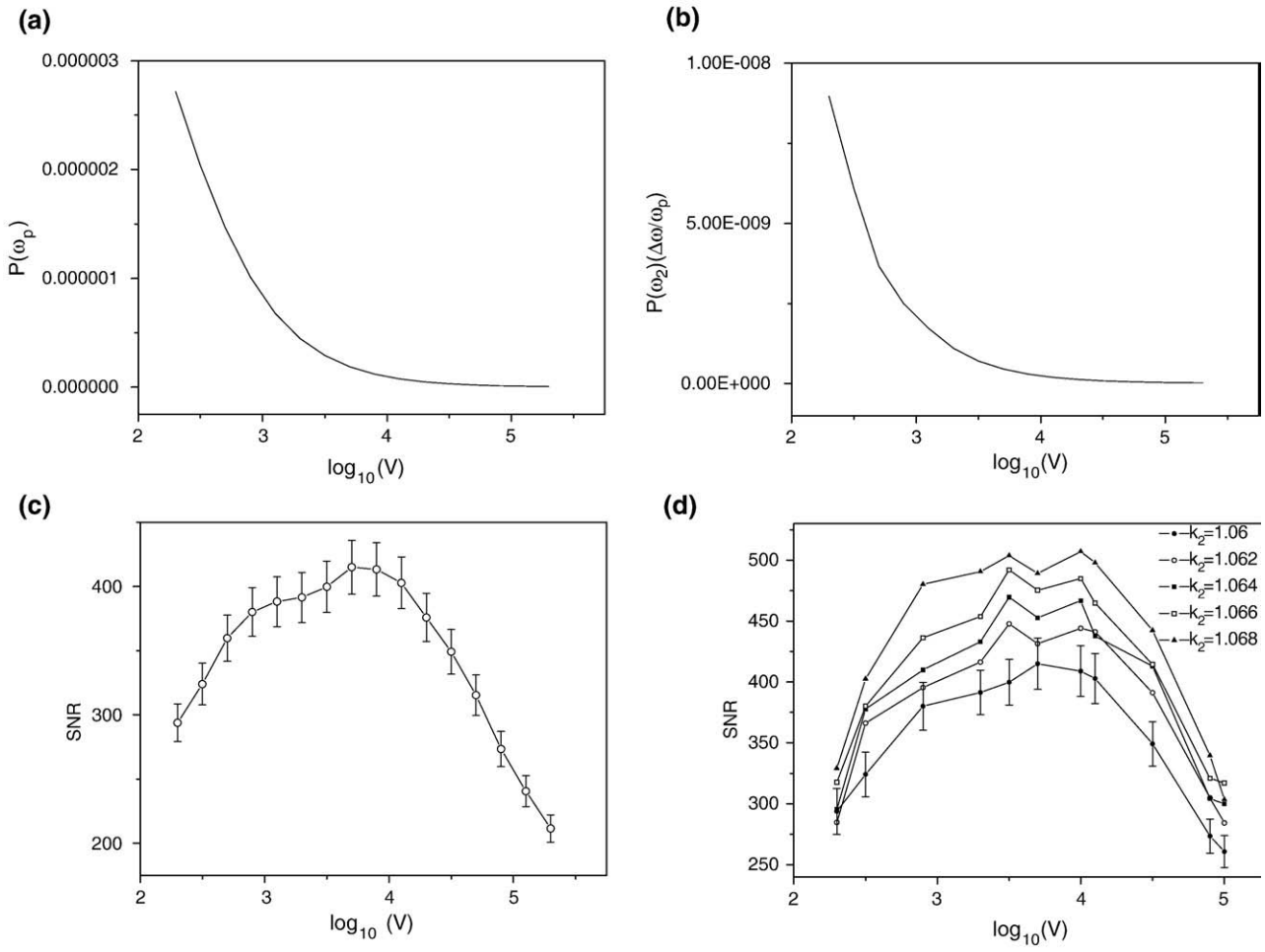

Fig. 3. (a) The dependence of the height of the peak $P(\omega_p)$ on V for y at $\hat{k}_2 = 1.06$. (b) The dependence of the quantity of $P(\omega_2)(\Delta\omega/\omega_p)$ on V for y at $\hat{k}_2 = 1.06$. (c) The dependence of SNR on V for y at $\hat{k}_2 = 1.06$. (d) SNR on V for different choices of k_2.

system still stays at the steady state. For small system size, the internal noise dominates the system, and the oscillatory behavior occurs. However, for the moderate system size (e.g. $\underline{V} = 10^4$ μm^3), the system shows stochastic calcium oscillations which appear to be periodic and distinct from random noise. It is confirmed by the peak in the power spectrum presented in Fig. 2d. This result suggests that internal noise has expanded the range of the control parameter over which the calcium system is oscillatory. Computationally, this is equivalent to letting the volume constant and changing the particle number in this volume plus adjusting the kinetic parameters [30].

To quantify the relative performance of the stochastic oscillations, signal-to-noise ratio (SNR) is defined in the same way as that in Ref. [33]. SNR $= R(\omega_p/\Delta\omega)$, where ω_p is the frequency at the peak, $\Delta\omega$ is the width between ω_p and the frequency ω_1 satisfying $\omega_1 > \omega_p$ and $P(\omega_1) = P(\omega_p)/e$, here $P(\cdot)$ denotes the power spectrum density (PSD) for a given frequency; $R = P(\omega_p)/P(\omega_2)$, where $P(\omega_2)$ is the smallest PSD value between $P(0)$ and $P(\omega_p)$. The dependence of the peak height $P(\omega_p)$ and the quantity of $P(\omega_2)(\Delta\omega/\omega_p)$ on $\underline{V}$ are shown in Fig. 3a–b. As the relative level of internal noise scales inversely with $\sqrt{V}$, Fig. 3c depicts how SNR and the quantities that influence SNR varies with $\underline{V}$. All SNR data are obtained by averaging 20 independent simulations, and each run is obtained by varying the seed number of internal noise. It is evident that there exists optimal internal noise intensity, corresponding to a certain system size, for which the peak of SNR is best resolved, thereby indicating the existence of SSR in the calcium system. In the present work the Hopf bifurcation is supercritical. Although the definition of SNR is different the height of the peak $P(\omega_p)$ and the quantity of $P(\omega_2)(\Delta\omega/\omega_p)$ monotonically decrease with the increment of the system size, i.e. with reduction of the internal noise, resulting in the resonant behavior. The results are in accordance with the generic ones in Ref. [37]. Notably, the maximum SNR appears at $\underline{V} \approx 10^{3.7}$ μm^3, which is on the same order as the real volume of living cells *in vivo* [19], implying that biological systems might have learned to exploit the internal noise to enhance its sensitivity. The SNR drops while the volume increases further as it is hard for the low level of internal noise at very large volumes to induce stochastic oscillations. The maximum SNR at a moderate volume

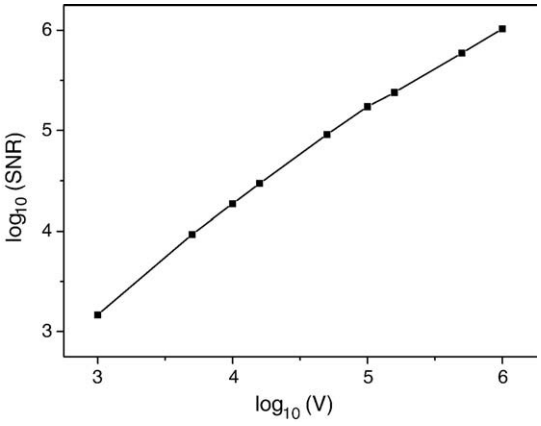

Fig. 4. The dependence of SNR on the system size V for y at $\hat{k}_2 = 1.3$.

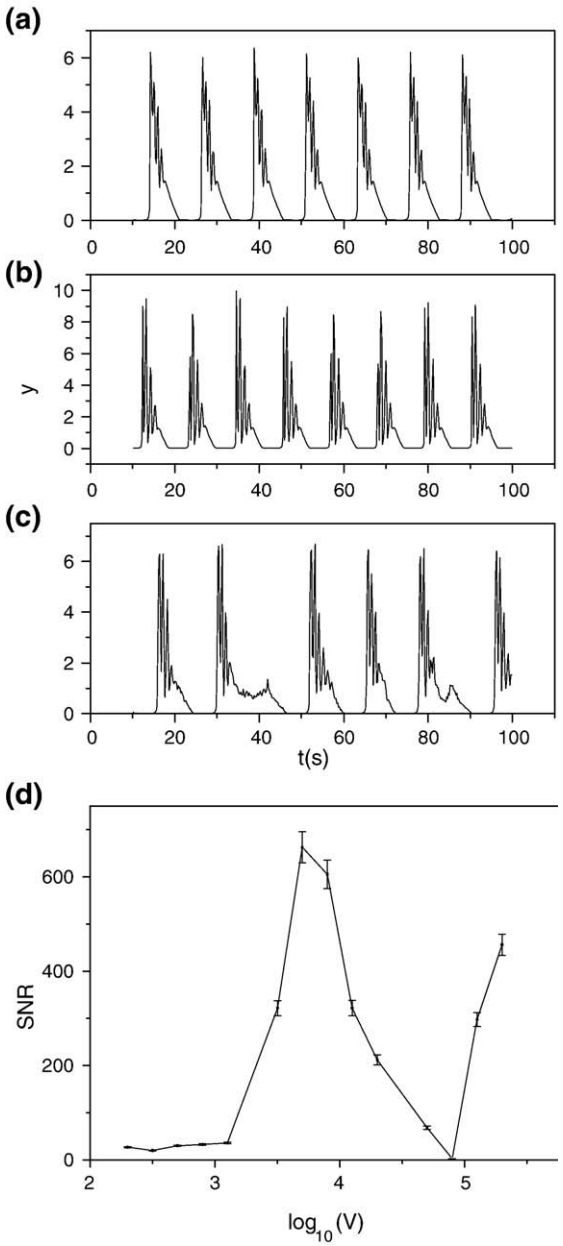

Fig. 5. Time series of calcium bursting for various volumes. (a) $V=10^6$ μm^3, (b) $V=10^4$ μm^3, (c) $V=10^3$ μm^3, (d) The dependence of SNR on V for y at $k_2=2.42$ in the bursting region.

indicates optimal calcium signaling. This calcium signal could be used for signaling and regulating the cell functions at a certain level of the agonist at which the deterministic models do not permit signaling. In addition, by using the CL method, how the SSR behavior depends on the control parameter k_2 was studied, as presented in Fig. 3d. The maxima of all these SNR curves are the fingerprints of the SSR behavior. As is seen from Fig. 3d, when the control parameter k_2 comes closer to the HB, the maximum SNR becomes larger. Li et al. has suggested a way of controlling internal signal stochastic resonance (ISSR) by varying the distance to the bifurcation point [38]. It is expected that the SSR could be controlled by the same way. Moreover, if the control parameter is tuned above the HB, e. g., $k_2=1.3$, SNR of the system increases monotonically with the augment of the cell volume, as is shown in Fig. 4, suggesting that internal noise plays destructive roles in the simple calcium oscillation region.

With further increase of k_2 the calcium system enters into the periodic bursting oscillation region, and the influence of internal noise on periodic bursting behavior was subsequently investigated. When the system size is large enough, e.g. $V=10^6$ μm^3, the simulation approaches the deterministic limit, as is displayed in Fig. 5a. Each main spike is succeeded by a series of secondary oscillations. As the system size decreases to $V=10^4$ μm^3, the oscillation grows faster due to the internal noise, as is shown in Fig. 5b. It is clearly in Fig. 5c that further decreasing the system size results in stochastic bursting oscillations, which are comparable to the experimental recordings [29]. The frequency of the main peak in the power spectrum is studied to see if SSR occurs in the bursting region. With varying the system size, SSR also appears in the periodic bursting region, as is demonstrated in Fig. 5d.

When k_2 is tuned to 1.06, which is close to HB, the frequency of calcium oscillation induced by the internal noise is invariable with increasing the system size. While in the burst region, the maximum frequency appears at $V=10^{3.7}$ μm^3, which contributes to SSR phenomenon. Secondly, the resonance is implicit in the steady state region, i.e., the oscillation is induced by internal noise and a maximum SNR is obtained at a moderate system size. SNR decreases endlessly with increasing the system size. Whereas in the periodic burst region, the resonance is explicit, i.e., the oscillation is inherence and a peak SNR is best resolved under the influence of internal noise. However, with further enhancement of the system size SNR cannot always reduce but begins to increase after $V=10^5$ μm^3 in that the simulation is approaching the deterministic limit. Thirdly, the peak SNR appears at the same system size $V=10^{3.7}$ μm^3 in the burst region and the steady state region.

As the SSR phenomenon is the focus in the present work, the two calcium subsystems are coupled unidirectionally to get more insight into its effect. The control parameters k_2 for the two subsystems are kept identical as 1.06, which are slightly lower than HB. As the behavior of the first subsystem is not affected and unchanged by the

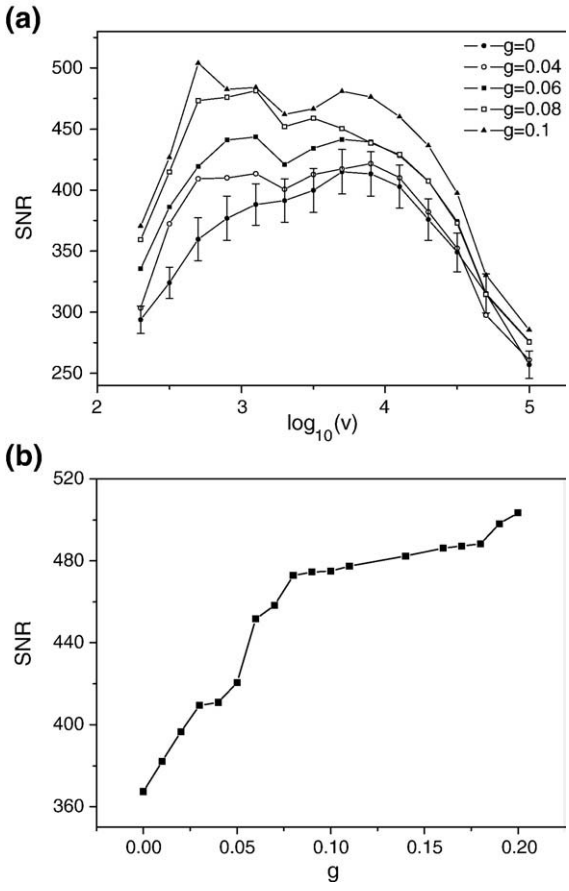

Fig. 6. (a) The dependence of SNR on the system size V for y_2 at different coupling strengths $g=0$, 0.04, 0.06, 0.08, and 0.1, respectively. (b) SNR for y_2 as the function of the coupling strength g at $V=10^3$ μm^3.

coupling, the second subsystem subject to the coupling is investigated accordingly. The SNR of $\underline{y_2}$ versus the cell volume for the second subsystem is presented in Fig. 6a which exhibits the corresponding SSR effect at various coupling levels. The SSR effect appears to be greater as the coupling strength increases from 0 to 0.1, indicating that coupling could significantly improve the SSR behavior of the subsystems exposed to internal noise. This is the reason that through coupling the information transfers from the former cell to the later cell via calcium signaling, and the information transmission is reinforced with the increase of the coupling strength. The dramatic increase of SNR for a small variation of coupling strength is apparent in Fig. 6a, suggesting that the system is sensitive to coupling. This phenomenon could be regarded as a sort of array-enhanced resonance. This suggests that biological systems might have made use of internal noise for intercellular calcium signaling by modulating coupling strength. The SNR of $\underline{y_2}$ at $\underline{V}=10^3$ μm^3 as a function of coupling strength is displayed in Fig. 6b, which clearly shows that the SNR increases monotonically with the coupling strength. Such a result further confirms that calcium oscillations are sensitive to coupling.

The array-enhanced resonance phenomenon has been observed in some unidirectionally coupled oscillators [15], where one subsystem (acts as the driver) is exposed to external noise. At certain coupling strength, synchronization appears among the coupled elements. In contrast to those studies, the small system size for the calcium system makes it necessary to adopt mesoscopic models due to the considerable internal noise, being an innate property of the system. Besides, different from previous work, the SNR increases monotonically with the coupling strength. These results might have implications for intercellular calcium signaling.

4. Conclusions

In the present work, the influence of internal noise originating from the random fluctuations due to finite size is studied in the calcium system. It is found that internal noise can induce stochastic oscillations while the corresponding deterministic system does not oscillate. The oscillations show the best regularity at a moderate volume, indicating the occurrence of system-size resonance. In the simple periodic oscillation region, however the internal noise plays a destructive role. In the complex oscillation region, e. g. the periodic bursting region, the presence of considerable internal noise makes the calcium oscillation in accordance with the experimental results. Additionally, the phenomenon of the SSR also appears in the periodic bursting regime due to the influence of internal noise. In a unidirectionally coupled calcium system, evidence is presented that coupling can significantly enhance system-size resonance behavior. This is different from the results reported in Ref. [15], where subsystems synchronized as the coupling strength exceeded a critical value. These findings are expected to be of importance toward the understanding of intracellular and intercellular calcium signaling.

Acknowledgments

The present work was supported by National Natural Science Foundation of China (Grant No. 20433050), and the 111 Project in China (B07012).

References

[1] J.W. Shuai, P. Jung, Optimal intracellular calcium signaling, Phys. Rev. Lett. 88 (2002) 068102.
[2] J.Q. Zhang, Z.H. Hou, H.W. Xin, System-size biresonance for intracellular calcium signaling, Chem. Phys. Chem. 5 (2004) 1041–1045.
[3] R. Thul, M. Fackle, Frequency of elemental events of intracellular Ca^{2+} dynamics, Phys. Rev. E 73 (2006) 061923.
[4] J. Paulsson, Summing up the noise in gene networks, Nature 427 (2004) 415–418.
[5] N. Baikai, S. Leibler, Circadian clocks limited by noise, Nature 403 (2000) 267–268.
[6] J.W. Shuai, P. Jung, Entropically enhanced excitability in small systems, Phys. Rev. Lett. 95 (2005) 114501.
[7] R.K. Adair, Noise and stochastic resonance in voltage-gated ion channels, Proc. Natl. Acad. Sci. U.S.A. 100 (2003) 12099–12104.
[8] A. Pikovsky, A. Zaikin, M.A. de la Casa, System size resonance in coupled noisy systems and in the Ising model, Phys. Rev. Lett. 88 (2002) 050601.
[9] H. Hong, B.J. Kim, M.Y. Choi, Optimal size of a complex network, Phys. Rev. E 67 (2003) 046101.
[10] R. Toral, C.R. Mirasso, J.D. Gunton, System size coherence resonance in coupled FitzHugh–Nagumo models, Europhys. Lett. 61 (2003) 162–167.
[11] P. Jung, J.W. Shuai, Optimal sizes of ion channel clusters, Europhys. Lett. 56 (2001) 29–35.
[12] J.W. Shuai, P. Jung, Optimal ion channel clustering for intracellular calcium signaling, Proc. Natl. Acad. Sci. U.S.A. 100 (2003) 506–510.
[13] J.W. Shuai, P. Jung, Stochastic properties of Ca^{2+} release of inositol 1,4,5-trisphosphate receptor clusters, Biophys. J. 83 (2002) 87–97.
[14] C.S. Zhou, J. Kurth, B. Hu, Array-enhanced coherence resonance: nontrivial effects of heterogeneity and spatial independence of noise, Phys. Rev. Lett. 87 (2001) 098101.
[15] Q.S. Li, Y. Liu, Enhancement and sustainment of internal stochastic resonance in unidirectional coupled neural system, Phys. Rev. E 73 (2006) 016218.
[16] B. von Haeften, R. Deza, H.S. Wio, Enhancement of stochastic resonance in distributed systems due to a selective coupling, Phys. Rev. Lett. 84 (2000) 404–407.
[17] J.M. Casado, Synchronization of two Hodgkin–Huxley neurons due to internal noise, Phys. Lett. A 310 (2003) 400–406.
[18] M.E. Gracheva, J.D. Gunton, Intercellular communication via intracellular calcium oscillations, J. Theor. Biol. 221 (2003) 513–518.
[19] M.E. Gracheva, R. Toral, J.D. Gunton, Stochastic effects in intercellular calcium spiking in hepatocytes, J. Theor. Biol. 212 (2001) 111–125.
[20] G. Dupont, T. Tordjmann, C. Clair, S. Swillens, M. Claret, L. Combettes, Mechanism of receptor-oriented intercellular calcium wave propagation in hepatocytes, FASEB J. 14 (2000) 279–289.
[21] M.J. Berridge, M.D. Bootman, P. Lipp, Calcium: a life and death signal, Nature 395 (1998) 645–648.
[22] A. Goldbeter, Computational approaches to cellular rhythms, Nature 420 (2002) 238–245.
[23] W.H. Li, J. Llopis, M. Whitney, G. Zlokarnik, R.Y. Tsien, Cell-permeant caged InsP3 ester shows that Ca^{2+} spike frequency can optimize gene expression, Nature 392 (1998) 936–941.
[24] R.E. Dolmetsch, K. Xu, R.S. Lewis, Calcium oscillations increase the efficiency and specificity of gene expression, Nature 392 (1998) 933–936.
[25] S. Schuster, M. Marhl, T. Höfer, Modelling of simple and complex calcium oscillations, Eur. J. Biochem. 269 (2002) 1333–1355.
[26] M. Marhl, T. Haberichter, M. Brumen, R. Heinrich, Complex calcium oscillations and the role of mitochondria and cytosolic protein, Biosystems 57 (2000) 75–86.
[27] U. Kummer, L.F. Olsen, C.J. Dixon, A.K. Green, E. Bornberg-Bauer, G. Baier, Switching from simple to complex oscillations in calcium signaling, Biophys. J. 79 (2000) 1188–1195.
[28] J.Q. Zhang, Z.H. Hou, H.W. Xin, Effects of internal noise for calcium signaling in a coupled cell system, Phys. Chem. Chem. Phys. 7 (2005) 2225–2228.
[29] U. Kummer, B. Krajnc, J. Pahle, A.K. Green, C.J. Dixon, M. Marhl, Transition from stochastic to deterministic behavior in calcium oscillations, Biophys. J. 89 (2005) 1603–1611.
[30] K.L. Davis, M.R. Roussel, Optimal observability of sustained stochastic competitive inhibition oscillations at organellar volumes, FEBS J. 273 (2005) 84–95.
[31] D.T. Gillespie, Exact stochastic simulation of coupled chemical reactions, J. Phys. Chem. 81 (1997) 2340–2361.
[32] D.T. Gillespie, The chemical Langevin equation, J. Chem. Phys. 113 (2000) 297–306.
[33] Z.H. Hou, H.W. Xin, Internal noise stochastic resonance in a circadian clock system, J. Chem. Phys. 119 (2003) 11508–11512.
[34] M. Yi, Y. Jia, Q. Liu, J.R. Li, C.L. Zhu, Enhancement of internal-noise coherence resonance by modulation of external noise in a circadian oscillator, Phys. Rev. E 73 (2006) 041923.
[35] Z.W. Wang, Z.H. Hou, H.W. Xin, Z.Z. Zhang, Engineered internal noise stochastic resonator in gene network: A model study, Biophys. Chem. 125 (2007) 281–285.
[36] D.J. Higham, An algorithmic introduction to numberical simulation of stochastic differential equations, SIAM Rev. 43 (2001) 525–546.
[37] O.V. Ushakov, H.-J. Wűnsche, F. Henneberger, I.A. Khovanov, L. Schimansky-Geier, M.A. Zaks, Coherence resonance near a Hopf bifurcation, Phys. Rev. Lett. 95 (2005) 123903.
[38] Y.P. Li, Q.S. Li, Implicit and explicit internal signal stochastic resonance in calcium ion oscillations, Chem. Phys. Lett. 417 (2006) 498–502.